ADVANCED HEALTHCARE MATERIALS
www.advhealthmat.de

Hydrogel Doped with Nanoparticles for Local Sustained Release of siRNA in Breast Cancer

Nathaly Segovia, Maria Pont, Nuria Oliva, Victor Ramos, Salvador Borrós, and Natalie Artzi**

Of all the much hyped and pricy cancer drugs, the benefits from the promising siRNA small molecule drugs are limited. Lack of efficient delivery vehicles that would release the drug locally, protect it from degradation, and ensure high transfection efficiency, precludes it from fulfilling its full potential. This work presents a novel platform for local and sustained delivery of siRNA with high transfection efficiencies both in vitro and in vivo in a breast cancer mice model. siRNA protection and high transfection efficiency are enabled by their encapsulation in oligopeptide-terminated poly(β-aminoester) (pBAE) nanoparticles. Sustained delivery of the siRNA is achieved by the enhanced stability of the nanoparticles when embedded in a hydrogel scaffold based on polyamidoamine (PAMAM) dendrimer cross-linked with dextran aldehyde. The combination of oligopeptide-terminated pBAE polymers and biodegradable hydrogels shows improved transfection efficiency in vivo even when compared with the most potent commercially available transfection reagents. These results highlight the advantage of using composite materials for successful delivery of these highly promising small molecules to combat cancer.

1. Introduction

RNA interference (RNAi) is a powerful tool for specific and efficient gene silencing of disease-related genes, which inhibits gene expression at the post-transcriptional level.[1] Therefore, RNAi has potential applications in biomedical research, in the treatment of cancer, skin disorders, infectious diseases or regenerative medicine.[1–5] New targets for RNAi-based cancer therapy have recently emerged, including specific RNAs targeting genes involved in proliferation, invasion, angiogenesis, metastasis, and chemo- and radiotherapy resistance. However, the delivery of siRNA is still an obstacle limiting the use and fulfillment of RNAi clinical potential.[6–9] Much effort focused on the development of vectors, either viruses or synthetic materials, capable of efficiently delivering therapeutic siRNAs into target cells.[10–13] While in vitro performance of vectors showed promising results, in vivo outcomes following systemic administration of such compounds have been modest, highlighting the limitations of such systems.

Local delivery of siRNA may overcome some of the limitations associated with systemic administration, with the intention of increasing anti-tumor activity and minimizing systemic toxicity.[3,9,14–17] Several approaches based on local and sustained delivery of active agents through hydrogel matrices have proved therapeutic benefits in vivo, including tumor suppression in melanoma and breast cancer models,[18] and angiogenesis promotion within tissue defects.[19] Poly(β-aminoester) (pBAE) polymers have emerged as efficient and biocompatible materials for the delivery of nucleic acids in gene therapy applications.[20,21] Recently, a new family of pBAE polymers containing terminal oligopeptides has been reported.[22] Nanoparticles prepared from nucleic acids and oligopeptide-terminated pBAE polymers achieve higher transfection efficiency and better cellular viability than other pBAE polymers and commercial transfection agents. This new family of pBAE polymers is promising for gene delivery due to their ability to condense nucleic acids into discrete nanoparticles facilitating cellular uptake, and to buffer the endosome allowing for endosomal escape. However, these polymers have limited applicability owing to rapid degradation via hydrolytic cleavage of ester bonds and thus cannot provide sustained delivery.

Injectable or implantable hydrogel scaffolds are increasingly used to locally and sustainably deliver therapeutic siRNAs, to increase the applicability of RNAi technology in cancer therapy.[19,23–25] Local administration of such systems, either in non-resectable tumors or in the tumor bed after surgical resection in combination with adjuvant regimens may be a superior alternative for providing increased survival rates of cancer patients.[26] Several hydrogel formulations based on chitosan,[11,18] fibrin,[27–29] hyaluronic acid,[4,28] gelatin[30] PEG,[31] or collagen[32] among others have been used as scaffolds for sustained delivery of DNA and siRNA nanoparticles. Although such systems have proved the feasibility of local and sustained delivery of nucleic acids, there are still several issues that need to be addressed, such as low siRNA stability, low transfection efficiency, and material-related toxicities.

N. Segovia, M. Pont, Dr. V. Ramos, Prof. S. Borrós
Grup d'Enginyeria de Materials (GEMAT)
Institut Quimic de Sarrià
Universidad Ramon Llul
Barcelona 08017, Spain
E-mail: salvador.borros@iqs.url.edu
M. Pont, N. Oliva, Prof. N. Artzi
Institute for Medical Engineering and Sciences
MIT, Cambridge 02139, MA, USA
E-mail: nartzi@mit.edu
Prof. N. Artzi
Department of Anesthesiology
Brigham and Women's Hospital
Harvard Medical School
Boston 02115, MA, USA

DOI: 10.1002/adhm.201400235

We hypothesized that the encapsulation of oligopeptide-terminated pBAE nanoparticles in a polymeric scaffold would provide siRNA protection, stabilization, and enhanced transfection. Particles fate would be extended and in large determined by the programmed degradation rate of the scaffold, enabling controlled siRNA release kinetics.

Recently, a novel hydrogel formulation with tissue-specific adhesion properties was developed based on poly(amido amine)-dextran aldehyde chemistry.[33] PAMAM:Dextran hydrogels can be easily obtained by spontaneous Schiff-base reaction between aldehyde groups of oxidized dextran and terminal amines of PAMAM dendrimers and serve as a scaffold for the embedment of siRNA-loaded particles. This adhesive hydrogel formulation has proved to be highly compatible, easy to obtain, injectable and tunable, making it an attractive material for local drug delivery applications.

In this work, a novel platform for local and sustained delivery of siRNA based on oligopeptide-terminated pBAE nanoparticles and PAMAM:Dextran hydrogel scaffolds was developed. We found that embedding of siRNA-pBAE nanoparticles in hydrogel scaffolds facilitates high and prolonged silencing efficiency both in vitro and in vivo in a murine breast cancer mouse model. The obtained results indicate that combination of oligopeptide-terminated pBAE polymers and biodegradable hydrogels is a powerful strategy to improve local administration of siRNA.

2. Results and Discussion

To overcome the limitations of systemic administration of nanoparticle-mediated siRNA, local delivery approach based on pBAE polymers embedded in an adhesive hydrogel was designed, as shown in **Figure 1**.

Arginine-terminated pBAE nanoparticles condense all the loaded siRNA (Figure S1, Supporting Information), and enable controlled release of the complexed-siRNA in a local and sustained manner as the hydrogel degrades.

2.1. In Vitro Transfection of Breast Cancer Cells with pBAE Nanoparticles

The silencing efficiency of siRNA nanoparticles fabricated with arginine-modified pBAE polymers was evaluated using MDA-MB-231 breast cancer cell line, stably expressing green fluorescent protein (GFP), using a specific anti-GFP siRNA (siGFP).

Transfection of MDA-MB-231 cells with arginine-modified pBAEs (R3C-C32-CR3) achieved higher silencing efficiencies compared with INTERFERin and Lipofectamine positive controls. Arginine-modified pBAEs showed 54% reduction in GFP fluorescence, and is the only group that exhibited statistical significant difference from untreated cells. In contrast, both commercial reagents showed 13% and 14% reduction in GFP fluorescence compared with untreated cells, respectively (**Figure 2**a). Cell viability analysis of positive controls, INTERFERin and Lipofectamine, showed cell survival of 100% and 75%, respectively, in agreement with the values provided by the supplier. Notably, arginine-modified pBAE polymers showed excellent cytocompatibility with cell viability of 96% (Figure 2b), in agreement with previously published data.[22]

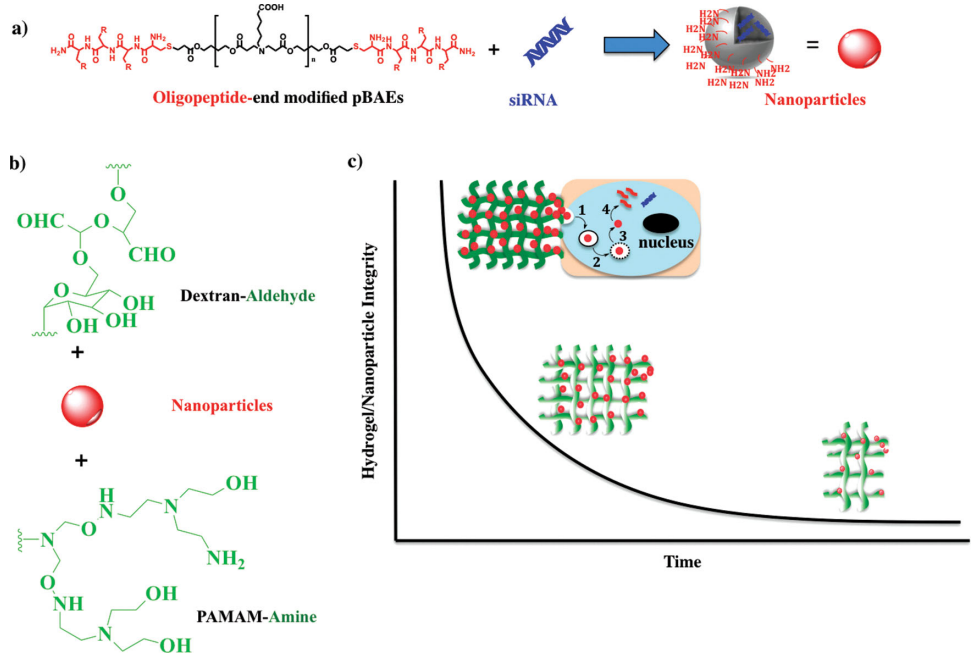

Figure 1. Schematic representation of sustained siRNA release from siRNA-loaded nanoparticles embedded in a polymeric scaffold: a) Oligopeptide-end-modified pBAEs condense siRNA into discrete nanoparticles, b) Hydrogel formation and in situ loading of siRNA nanoparticles, c) Hydrogel/nanoparticle disintegration with time, and transfection process: 1) cellular uptake of nanoparticles by endocytosis, 2) buffering capacity and 3) subsequent endosomal escape, and 4) siRNA dissociation from the nanoparticle.

DOI: 10.1002/adhm.201400235

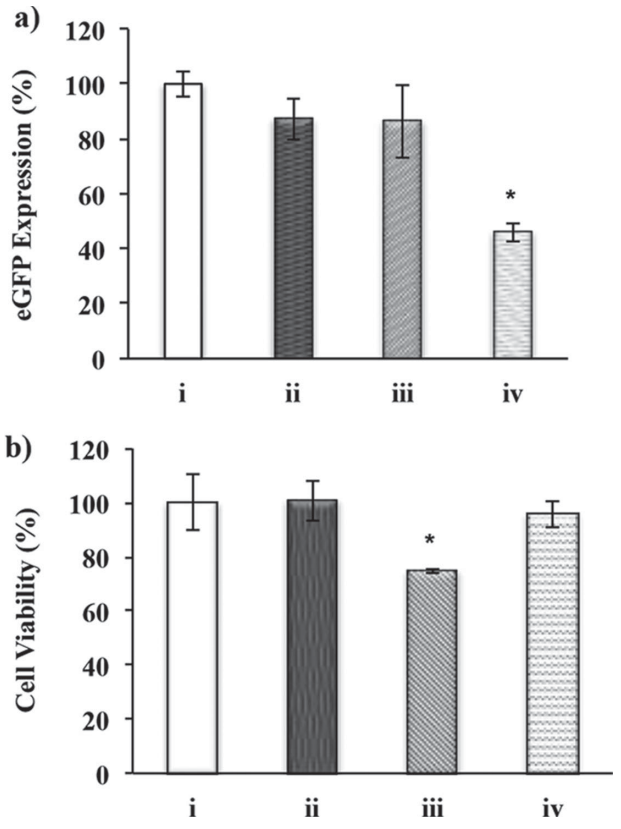

Figure 2. Gene silencing and cell viability of MDA-MB-231-GFP cells, transfected with different pBAE polymer nanoparticles. MDA-MB-231-GFP cells were transfected with siGFP pool at a final concentration of 25×10^{-9} M of siGFP/well. i) Untreated cells, ii) Polyplus, iii) Lipofectamine, and iv) Arginine-modified pBAEs. a) GFP silencing was analyzed 48 h post-transfection by flow cytometry. Numbers above each bar represent the average percentage of GFP expression relative to a control of untreated cells.b) Cell viability assay was performed 48 h post-transfection using MTS assay. Viability was plotted as percentage of viable cells relative to a control of untreated cells. Results are shown as mean and standard deviation of triplicates. Statistical significance was determined using untreated cells as control, $*p < 0.05$.

2.2. Incorporation of Nanoparticles into the Hydrogel

Given the excellent silencing efficiency and cytocompatibility of siRNA-pBAE nanoparticles, particles were encapsulated in biodegradable PAMAM:Dextran hydrogels via in situ loading into dextran solution prior to injection and hydrogel formation. Different concentrations of siRNA nanoparticles loaded into the hydrogels did not significantly affect hydrogel properties, including hydrogel gelation time and morphology (Figure S2, Supporting Information). Alexafluor-647-labeled siRNA and fluorescein-labeled PAMAM were used to fluorescently image the nanoparticles in the hydrogel (**Figure 3**).

Fluorescence microscopy images showed homogeneous distribution of the siRNA nanoparticles in the hydrogel network. The dual labeling reveals colocalization of the nanoparticles and the polymeric matrix along with particles distributed within the pores. These results suggest that in addition to the physical entrapment of the nanoparticles within the hydrogel matrix, chemical interaction between aldehyde groups from

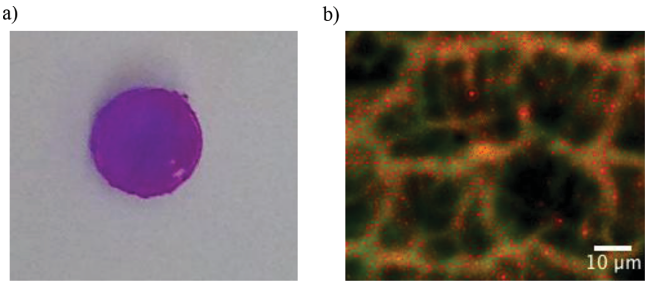

Figure 3. siRNA nanoparticles are well distributed within the hydrogel scaffold. a) 6 mm diameter, 3 mm thick fluorescently-labeled hydrogel. b) Amplified fluorescent microscopy image of hydrogel doped with siRNA encapsulated into arginine-modified pBAEs nanoparticles (1.2 μg siRNA/100 μL hydrogel). PAMAM is labeled with fluorescein (green) and siRNA is labeled with Alexafluor-647 (red). Pore size is 45 ± 6 μm.

oxidized dextran and amine groups present on the nanoparticle surface takes place.

2.2.1. siRNA Release Kinetics is Sustained when Embedded in the Hydrogel

In order to understand the mechanisms that govern siRNA release kinetics from the scaffold, both nanoparticle and hydrogel degradation were studied. Fluorescein-labeled nanoparticles were incorporated into the hydrogel and then incubated in phosphate buffer saline (PBS) solution at 37 °C for 13 d. Nanoparticles degradation was followed by tracking the loss of fluorescence intensity over time, and stability assessed by nanoparticle tracking analysis (NTA) (**Figure 4**a). Nanoparticles alone were fast degrading via hydrolytic cleavage of the ester groups of pBAE polymers. In the first 7 h, approximately 60% of nanoparticles were degraded and full degradation occurred by 24 h, precluding these particles from clinical use. In contrast, the rate of nanoparticle degradation inside the hydrogel was significantly reduced. Nanoparticles release and degradation followed two phases. The first phase comprised of rapid release of approximately 50% of the particles, followed by a more sustained release reaching 100% after 12 d. The initial fast nanoparticle release results from the wash out of physically entrapped nanoparticles upon material swelling, providing the first bolus release. This is followed by sustained release of the particles upon hydrogel degradation, which is more gradual. This phenomenon indicates that immobilization of nanoparticles onto the hydrogel network was beneficial to nanoparticle stabilization, promoted by the caging and cross-linking effect of the oxidized dextran, which provided stabilization of siRNA-pBAE polyplexes, similarly as described in earlier studies.[27,34,35] To further prove that the aminated particles interact with dextran aldehyde and in that way provide retention in the hydrogel, we allowed the nanoparticles to interact with the dextran solution for 5 min prior to injection and hydrogel formation upon mixing with PAMAM dendrimer, instead of immediately injecting the hydrogel. This enables the aminated particles to interact with aldehyde groups on the dextran while removing the competing reaction of dendrimer amines with dextran aldehydes. This indeed results in slower release of the particles from the hydrogel (Figure S3,

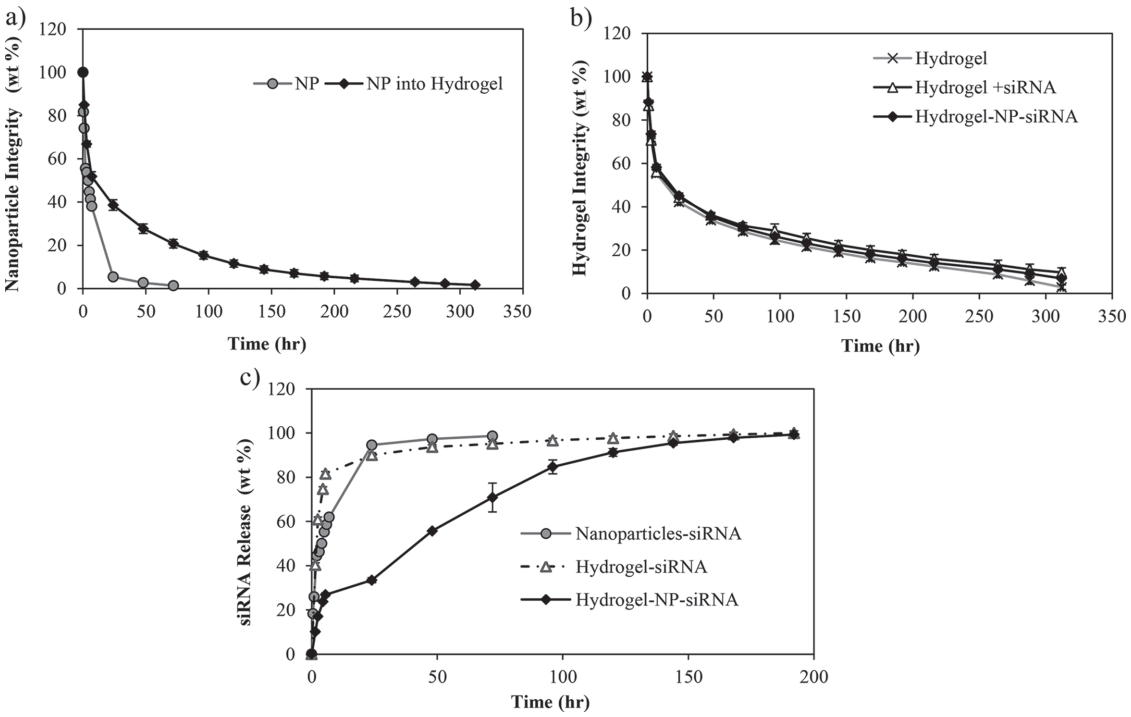

Figure 4. In vitro release kinetics of siRNA embedded in hydrogel matrices. a) In vitro degradation profile of nanoparticles based on oligopeptide-modified pBAEs in phosphate buffer saline 1× at 37 °C. Nanoparticles were labeled with fluorescein and degradation was followed by tracking the loss of fluorescence with time. b) In vitro degradation profile of PAMAM:Dextran (6.25%:5%, w/v) hydrogel followed by tracking the loss of fluorescence with time (Alexafluor-594). c) In vitro release of siRNA-Alexafluor-647 from the hydrogel, the nanoparticles, or their combination. Results are shown as mean and standard deviation of triplicates.

Supporting Information), proving that the particles react with the adhesive scaffold. To examine the release in the absence of chemical interaction, we embedded in the scaffold control polystyrene beads, with identical size to that of our synthesized siRNA-containing nanoparticles, but incapable of chemical binding to the hydrogel, and followed their release. In the absence of chemical interaction, the particles burst out almost immediately (Figure S3, Supporting Information).

The influence of nanoparticle incorporation into the hydrogel on scaffold degradation kinetics was evaluated. Hydrogel degradation profiles were determined for hydrogel alone, hydrogel containing either free or encapsulated siRNA abbreviated as hydrogel-siRNA and hydrogel-NP-siRNA, respectively. PAMAM:Dextran hydrogels degradation was followed by tracking the loss of fluorescence intensity with time using fluorescently-labeled dextran (Figure 4b). Hydrogel degradation was not affected by nanoparticle incorporation as degradation profile for both hydrogel-siRNA and hydrogel-NP-siRNA exhibited the same degradation kinetics. In the first 24 h, hydrogel degradation was rapid with 65% erosion, followed by a slower degardation that is completed after 12 d.

Finally, siRNA release from the hydrogel for either free siRNA or siRNA nanoparticles was determined by tracking the fluorescent intensity of fluorescently-labeled siRNA over time (Figure 4c). Free uncomplexed siRNA showed rapid release of 90% within 24 h, in agreement with literature reports.[23,24,36,37] Interestingly, these results were similar to the stability observed for siRNA nanoparticles alone, where complete siRNA release occurred within 24 h.

In contrast, siRNA nanoparticles embedded in the scaffold showed a significantly slower release. In the first 24 h, 30% of siRNA was released, followed by more gradual release reaching 90% by day 6 of physically entrapped and covalently attached particles, respectively.

2.2.2. Deciphering the Mechanism of siRNA Release when Hydrogel Embedded

To understand the mechanism that controls the release of both uncomplexed- and complexed-siRNA from the scaffold, siRNA release versus hydrogel degradation was graphically represented. Uncomplexed siRNA encapsulated inside the scaffold showed fast siRNA release profile; by the time 55% of the hydrogel degraded, over 81% of siRNA was released from the scaffold in contrast to 33% of complexed-siRNA release. When over 60% of the hydrogel degraded, siRNA release kinetics was enhanced, due to the loss of hydrogel structural integrity. siRNA release from the nanoparticles was slower than that in the hydrogel alone, as the former follows nanoparticles surface erosion while the latter occurs immediately upon hydrogel swelling (**Figure 5**).

Given that hydrogel degradation profiles with and without siRNA are identical, the fast release obtained when uncomplexed-siRNA was incorporated to the hydrogel suggests that siRNA was only physically entrapped in the hydrogel, therefore it could easily diffuse out upon hydrogel swelling. In contrast, complexed-siRNA embedded in the scaffold showed a

Adv. Healthcare Mater. **2014**,
DOI: 10.1002/adhm.201400235

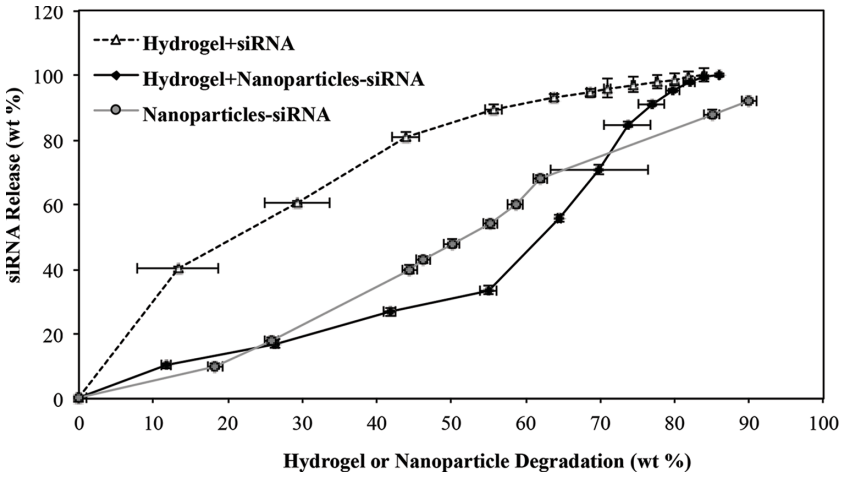

Figure 5. In vitro siRNA release as a function of hydrogel degradation. Gradual siRNA release is obtained when siRNA is encapsulated and embedded in the hydrogel, compared with the fast release when either embedded (PAMAM:dextran 6.25%:5%, w/v) or encapsulated. Results are shown as mean and standard deviation of triplicates.

sustained release over a longer period of time compared with uncomplexed-siRNA a result of: 1) higher retention and stability of nanoparticles when embedded in the hydrogel matrix due to chemical interaction between the nanoparticles and the hydrogel matrix, 2) higher retention and stability of siRNA when encapsulated by the nanoparticles that provides protection from degradation, and 3) slow diffusion rate of the large unbound polyplexes compared with free siRNA and need for chemical degradation to occur when the particles are bound to dextran. Hence, the biphasic release of siRNA encapsulated in the particles and in the hydrogel suggests that during the first phase, physically entrapped nanoparticles are quickly released upon polymer swelling, resulting in a fast release of siRNA in the first phase, followed by a second phase of release of the particles that are chemically bound to the hydrogel following imine bond cleavage between dextran aldehyde and nanoparticles surface amines. The integrity of the released siRNA was confirmed by gel retardation assay of the complexed particles in the medium (Figure S4, Supporting Information).

2.3. In Vitro Silencing Efficiency of GFP Expression with Hydrogel Embedded siRNA-pBAE Nanoparticles

To determine the potential of hydrogels to deliver bioactive nanoparticles, gene silencing and cell viability were assessed in vitro. Silencing capacity of anti-GFP siRNA toward MDA-MB-231 breast cancer cells stably expressing green fluorescent protein was evaluated for hydrogels loaded with siRNA nanoparticles, siRNA nanoparticles alone or free siRNA entrapped in hydrogel. Polyplus, a commercial reagent, was used as a positive control, while negative controls included untreated cells and cells embedded within hydrogels. Both GFP silencing efficiency and cell viability were determined at 3 d post-transfection by flow cytometry and MTS assay, respectively (**Figure 6**a,b).

Analysis of cell fluorescence revealed that incubation of GFP-expressing cells with hydrogels containing siRNA nanoparticles achieved a significant GFP silencing, up to 55% knockdown in fluorescence. However, gene silencing was not observed in hydrogels embedded with uncomplexed siRNA, which confirmed that siRNA from nanoparticle--hydrogel formulations was released in the form of active nanoparticles capable of transfecting cells. Knock-down efficiency of free nanoparticles suspension compared with nanoparticles entrapped within the hydrogel matrix was 76% versus 55%, respectively. Taking into account that the siRNA released from nanoparticle-loaded hydrogels after 72 h reached approximately 70% of the total siRNA loaded in the scaffold (see Figure 4c), the obtained results are in agreement with the amount of siRNA released and available in the culture medium.

Assessment of cell viability after transfection revealed that our hydrogel is cytocompatible, since cells incubated with either hydrogel or hydrogel-containing siRNA show cell viabilities greater than 85%, when compared with untreated cells. Hydrogel scaffolds containing siRNA nanoparticles had satisfactory cell viability, over 65%, when compared with untreated cells. The modest decrease in cell viability seen when hydrogels are loaded with siRNA nanoparticles compared with hydrogel or siRNA-pBAE nanoparticles alone may result from the transfection itself.

2.4. In Vivo Silencing of Luciferase-Expressing Tumors via Sustained siRNA Delivery from Hydrogel Scaffolds

The performance of hydrogel scaffolds loaded with anti-luciferase siRNA nanoparticles (siLuc nanoparticles) was tested in vivo in xenograft mouse model of human breast cancer.[38] Luciferase-expressing MDA-MB-231 tumor cells were injected into the mammary fat pad of SCID mice and tumors were allowed to develop. Once tumors reached a desired volume (150 mm^3), fluorescently-labeled scaffolds loaded with siLuc nanoparticles were implanted adjacent to the mammary fat pad tumor. Silencing efficiency of luciferase expression and hydrogel stability were determined at different time points by bioluminescence imaging and fluorescence monitoring, respectively. Control sample of JetPEI-siLuc was injected intratumorally. Tumor-associated luciferase expression was monitored over a period of 6 days following luciferin injection (**Figure 7**).

All mice maintained healthy appearance after scaffold implantation and inflammation was not observed at the surgical site, suggesting that hydrogels did not exert material-related toxicity. Bioluminescence imaging of mice revealed that scaffolds were able to promote efficient and sustained luciferase silencing over the course of the study, reaching up to 70% reduction in luciferase expression after 6 d. In contrast, nanoparticles injected intratumorally achieved a maximum reduction in luciferase expression of 20% during the same period of time. Statistical analysis confirmed that reduction of luciferase

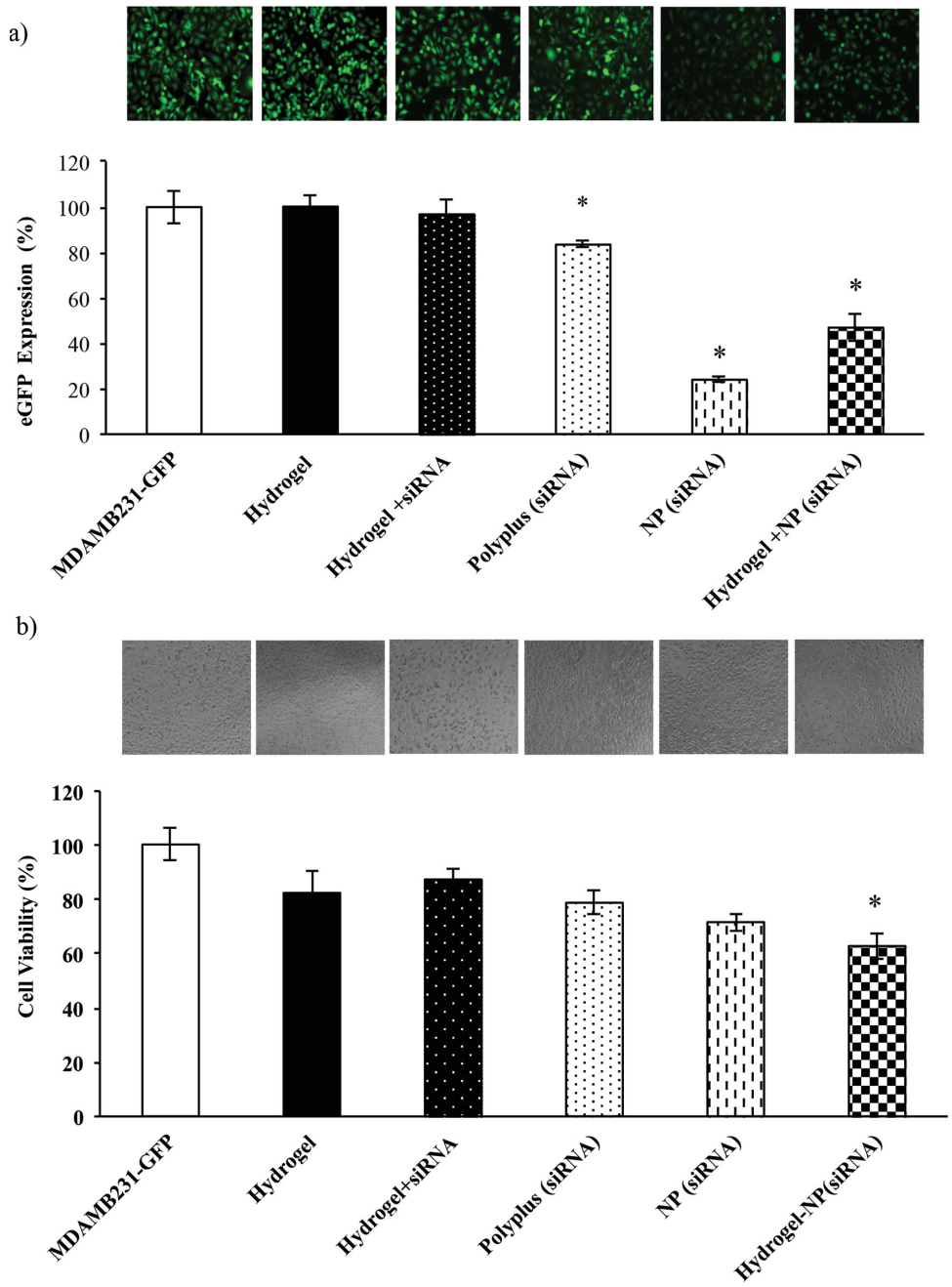

Figure 6. In vitro assessment of gene silencing efficiency and cell viability of hydrogels containing embedded siRNA-pBAE nanoparticles. In vitro transfection using siGFP was performed using MDA-MB-231-GFP cells stably expressing green fluorescent protein. Negative controls: untreated MDA-MB-231-GFP cells and hydrogel; Hydrogel + siRNA: hydrogel containing free siRNA at 2 μg siRNA/disc; Positive control: polyplus at siGFP concentration of 25×10^{-9} M per well; NP(siRNA): nanoparticles (CR3-C32-CR3:siGFP at ratio 200:1 w/w) at concentration of 25×10^{-9} M siGFP per well; Hydrogel-NP(siRNA): hydrogel doped with nanoparticles (CR3-C32-CR3:siGFP at ratio 200:1 w/w). a) GFP silencing was analyzed after 72 h post-transfection by flow cytometry. Percentage values above each bar represent the average percentage of EGFP expression relative to a control of untreated cells. Results are shown as mean and standard deviation of triplicates. Statistical significance was determined using MDA-MB-231-GFP cells as control group, $^*p < 0.05$. b) Cell viability assay was performed at 72 h post-transfection using MTS assay. Cell viability was calculated as percentage of viable cells relative to a control of untreated cells. Results are shown as mean and standard deviation of triplicates. Statistical significance was determined using polyplus as control group, $^*p < 0.05$.

expression achieved with hydrogel scaffold was significantly different compared with negative control and Jet-PEI (commercial reagent). These in vivo results confirmed that the released nanoparticles were bioactive, allowing luciferase silencing over prolonged periods of time (Figure 7a,b).

In addition, hydrogel degradation was followed in vivo to study whether hydrogel fate drives luciferase gene silencing. Hydrogel degradation was calculated from fluorescence signals in the region of interest around the tumor (Figure S5, Supplementary Information).

Adv. Healthcare Mater. **2014**,
DOI: 10.1002/adhm.201400235

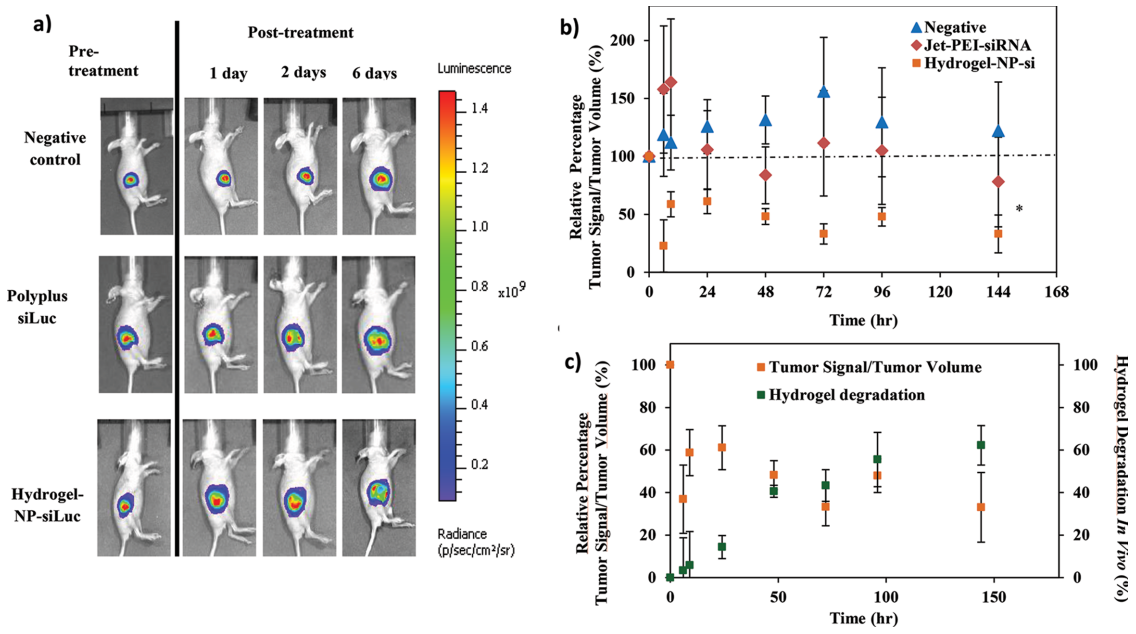

Figure 7. Prolonged in vivo silencing of luciferase-expressing tumors using hydrogel scaffold loaded with siLuc nanoparticles. a) Silencing of luciferase-expressing tumors was achieved 24 h post-treatment and maintained until 6 d post-treatment. Negative control: tumor alone; Positive control: tumor treated with siLuc encapsulated with a commercial reagent (Jet-PEI, Polyplus) at a dose of 10 μg siRNA/tumor; Hydrogel-NP-siLuc: tumor treated with hydrogel doped with nanoparticles containing siLuc at a dose of 10 μg siRNA/tumor.b) Quantification of luciferase expression in tumors treated with siLuc. Results are shown as mean and standard deviation of replicates ($n = 5$). Statistical significance was determined between sets of measurements, $^*p < 0.05$. Hy-NP-siLuc signal was significantly different from both negative and positive controls.c) Relationship between luciferase expression in tumors and hydrogel degradation in mice treated with Hy-NP-siLuc.

Interestingly, in vivo hydrogel degradation showed good correlation with luciferase silencing as release of siLuc nanoparticles increased with hydrogel degradation. In the first 72 h, hydrogel scaffolds were degraded approximately 43% and luciferase expression was reduced to 54%, when compared with negative control. After 72 h, hydrogel degradation increased, while luciferase expression further decreased and its low expression maintained over time. The highest value of luciferase silencing coincided with the highest value of hydrogel degradation at day 6, achieving values over 70% and 60%, respectively (Figure 7c). During the first 6 h, high silencing efficiency was observed, where only 3% of hydrogel was degraded, possibly due to a burst release of physically entrapped siRNA-encapsulated nanoparticles from the scaffold.

To the best of our knowledge, previous reports showed efficient in vivo knockdown only following two consecutive applications of siRNA and when accompanied by commercial transfection reagents like Lipofectamine 2000[39] or PEI[40] to improve cell uptake. Previous studies did not exhibit significant silencing efficiencies after 7 d post-scaffold implantation.[19] Future work will examine the ability to further tune the release kinetics of the particles from the hydrogel, especially the initial rapid release, by tuning hydrogel formulation. We will then utilize this versatile platform to deliver specific siRNAs like EGFR, along with chemotherapeutic agents.

3. Conclusions

Development of local delivery systems would increase the applicability of RNAi technology in multiple localized or compartmentalized diseases. The availability of a vast number of polymeric scaffolds that are biocompatible and whose degradation kinetics can be programmed should be exploited for siRNA local delivery. This will facilitate high concentration of siRNA at the target site while minimizing off-target effects. Here, a new delivery platform has been developed by embedding siRNA-encapsulated nanoparticles capable of transfection and endosomal escape in an adhesive hydrogel scaffold that provides siRNA protection and sustained release. The cell compatibility and tunability of the hydrogel scaffold together with the high transfection efficiency of the oligopeptide-modified poly(β-aminoester) nanoparticles make it an attractive platform that can either complement or in some cases replace systemic delivery. The results obtained in this work have demonstrated efficient and sustained release of siRNA in a breast cancer model and represent an opportunity for further development of cancer RNAi therapeutics.

4. Experimental Section

Synthesis of Oligopeptide-modified pBAEs Polymers: Poly(β-aminoester)s were synthesized following a two-step procedure previously described in the literature. First, an acrylate-terminated polymer was synthesized by addition reaction of primary amines with diacrylates (at 1:1.2 molar ratio of amine:diacrylate). Briefly, 5-amino-1-pentanol (3.44 g, 33 mmol) and 1,4-butanediol diacrylate (7.93 g, 40 mmol) were polymerized at 90 °C for 24 h. Oligopeptide-modified pBAEs were obtained by end-capping modification of the resulting acrylate-terminated polymer with thiol-terminated oligopeptide at 1:2.1 molar ratio in dimethyl sulfoxide. The mixture was stirred overnight at room temperature and the resulting

polymer was obtained by precipitation in a mixture of diethyl ether and acetone (1:1). Synthesized structures were confirmed by ^{1}H NMR and FTIR analysis. NMR spectra were recorded in a 400 MHz Varian (Varian NMR Instruments, Claredon Hills, IL, USA) and methanol-d_4 was used as solvent. IR spectra were obtained using a Nicolet Magna 560 (Thermo Fisher Scientific, Waltham, MA, USA) with a KBr beamsplitter, using methanol as solvent in evaporated film. Molecular weight determination was conducted using a Hewlett-Packard 1050 Series HPLC system equipped with two GPC Ultrastyragel columns, 10^3 and 10^4 Å (5 µm mixed, 300 mm × 19 mm, Waters Millipore Corporation, Milford, MA, USA) and THF as mobile phase. The molecular weight was calculated by comparison with the retention times of polystyrene standards.

R3C-C32-CR3IR (Evaporated Film): ν = 721, 801, 834, 951, 1029, 1133 (C—O), 1201, 1421, 1466, 1542, 1672 (C═O, from peptide amide), 1731 (C═O, from ester), 2858, 2941, 3182, 3343 (N—H, O—H) cm^{-1}.^{1}H NMR (400 MHz, CD_3OD, TMS) (ppm): δ = 4.41–4.33 (br, NH_2—C(═O)—CH—NH—C(═O)—CH—NH—C(═O)—CH—NH—C (═O)—CH—CH_2—, 4.11 (t, CH_2—CH_2—O), 3.55 (t, CH_2—CH_2—OH), 3.22 (br, NH_2—C(═NH)—NH—CH_2—, OH—$(CH_2)_4$—CH_2—N—), 3.04 (t, CH_2—CH_2—N—), 2.82 (dd, —CH_2—S—CH_2), 2.48 (br, —N—CH_2—CH_2—C(═O)—O), 1.90 (m, NH_2—C(═NH)—NH—$(CH_2)_2$—CH_2—CH—), 1.73 (br, —O—CH_2—CH_2—CH_2—CH_2—O), 1.69 (m, NH_2—C(═NH)—NH—CH_2—CH_2—CH_2—), 1.56 (br, —CH_2—CH_2—CH_2—CH_2—OH), 1.39 (br, —N—$(CH_2)_2$—CH_2—$(CH_2)_2$—OH).

K3C-C32-CK3IR (Evaporated Film): ν = 721, 799, 834, 1040, 1132, 1179 (C—O), 1201, 1397, 1459, 1541, 1675 (C═O, from peptide amide), 1732 (C═O, from ester), 2861, 2940, 3348 (N—H, O—H) cm^{-1}. ^{1}H NMR (400 MHz, CD_3OD, TMS) (ppm): δ = 4.38–4.29 (br, NH_2—$(CH_2)_4$—CH—), 4.13 (t, CH_2—CH_2—O—), 3.73 (br, NH_2—CH—CH_2—S—), 3.55 (t, CH_2—CH_2—OH), 2.94 (br, CH_2—CH_2—N—, NH_2—CH_2—$(CH_2)_3$—CH—), 2.81 (dd, —CH_2—S—CH_2), 2.57 (br, —N—CH_2—CH_2—C(═O)—O), 1.85 (m, NH_2—$(CH_2)_3$—CH_2—CH—), 1.74 (br, —O—CH_2—CH_2—CH_2—CH_2—O), 1.68 (m, NH_2—CH_2—CH_2—$(CH_2)_2$—CH—), 1.54 (br, —CH_2—CH_2—CH_2—CH_2—OH), 1.37 (br, —N—$(CH_2)_2$—CH_2—$(CH_2)_2$—OH).

H3C-C32-CH3IR (Evaporated Film): ν = 720, 799, 832, 1040, 1132, 1201, 1335, 1403, 1467, 1539, 1674 (C═O, from peptide amide), 1731 (C═O, from ester), 2865, 2941, 3336 (N—H, O—H) cm^{-1}. ^{1}H NMR (400 MHz, CD_3OD, TMS) (ppm): δ = 8.0–7.0 (br, —N(═CH)—NH—C(═CH)—), 4.61–4.36 (br, —CH_2—CH—), 4.16 (t, CH_2—CH_2—O—), 3.55 (t, CH_2—CH_2—OH), 3.18 (t, CH_2—CH_2—N—, 3.06 (dd, —CH_2—CH—), 2.88 (br, OH—$(CH_2)_4$—CH_2—N—), 2.82 (dd, —CH_2—S—CH_2—), 2.72 (br, —N—CH_2—CH_2—C(═O)—O), 1.75 (br, —O—CH_2—CH_2—CH_2—CH_2—O), 1.65 (m, NH_2—CH_2—CH_2—$(CH_2)_2$—CH—), 1.58 (br, —CH_2—CH_2—CH_2—CH_2—OH), 1.40 (br, —N—$(CH_2)_2$—CH_2—$(CH_2)_2$—OH).

Formation of Polymer/siRNA Nanoparticles: Polyplexes were freshly prepared before use. Stock solutions of pBAEs in DMSO (100 mg mL^{-1}) were diluted with water and appropriate amounts of polymer solution were added to siRNA solution in equal volumes to obtain polymer/siRNA polyplexes at 200:1 ratio (w/w). Polyplexes were mixed under vigorous vortexing for a few seconds, and incubated at room temperature for 30 min.

Synthesis and Formation of PAMAM:Dextran Hydrogels: The synthesis of dextran aldehyde as well as the PAMAM:Dextran hydrogel formation have been previously described.[3] Briefly, generation five polyamidoamine (PAMAM) dendrimer with 25% amine surface groups (Dendritech Inc.) was dissolved in water to obtain a 12.5% (w/v) aqueous solution. Linear dextran (10 kDa) was oxidized with sodium periodate to yield dextran aldehyde (50% oxidation of glucose rings, two aldehydes groups per oxidized glucose ring), which was also prepared as an aqueous solution (10%, w/v). The two homogeneous polymer solutions were mixed in equal volumes by pipetting and network formation occurred within seconds by Schiff-base reaction between the constituent reactive groups (aldehydes and amines).

Formation of PAMAM:Dextran Hydrogels Doped with Free siRNA and Hydrogel Doped with Nanoparticles Encapsulating siRNA: PAMAM and dextran aqueous solutions were prepared as described before. In a sterile tube, dextran aldehyde solution (40 µL, 12.5%, w/v) was mixed with an siRNA solution or with nanoparticle solution (20 µL in water, at the desired concentration of siRNA), by gentle pipetting. Next, PAMAM solution (40 µL, 15.6%, w/v) was added and mixed by pipetting and subsequently loaded into rubber mold sandwiched between two glass slides (6 mm diameter, 3 mm thick disk) to obtain hydrogel doped with free siRNA or hydrogel doped with siRNA encapsulated into the nanoparticles, respectively.

Pore Size Analysis: Fluorescently-labeled dendrimer:dextran solutions were injected using a dual-barrel syringe into a mold to form a labeled-hydrogel disk doped with siRNA nanoparticles. Dextran solution (40 µL, 12.5%, w/v) was mixed with Alexafluor-647-labeled-siRNA nanoparticle solution (20 µL). PAMAM aqueous solution containing 2% fluorescein-labeled dendrimer (40 µL, 15.6%, w/v) was loaded to the second barrel. Following injection, the two solutions mixed and formed a gel. The gel was allowed to freeze overnight and then was cryosectioned (16 µm section) for visualization using fluorescence microscopy (LEICA DMRA2 epifluorescence microscope coupled with a Hamamatsu CA 4742–95 camera). Hydrogel pore size was determined using image analysis software (Fiji software) of the fluorescent images.

In Vitro Release Study of Alexafluor-647-Labeled siRNA from PAMAM:Dextran Hydrogel: Hydrogel doped with free Alexafluor-647-labeled siRNA (QIAGEN) or doped with Alexafluor-647-labeled siRNA encapsulated into the nanoparticles was prepared as described before at a dose of 2 µg siRNA/disk. Disks were incubated with PBS solution in 48 well plates at 37 °C for 10 d. At predetermined time points, the supernatant was completely removed (250 µL) and replaced with fresh PBS solution (250 µL). The fluorescent signal of the labeled siRNA (siRNA-Alexafluor-647) was used to quantify siRNA release. The percentage was calculated based on the amount released at a given time point relative to the amount loaded.

In Vitro Degradation Study of Nanoparticles Encapsulated into the PAMAM:Dextran Hydrogels: Fluorescein-labeled nanoparticles were formed by mixing a pBAEs solution containing 10% fluorescein-labeled pBAEs with siRNA (siGFP pool) as described before. Fluorescein nanoparticles were incorporated into the hydrogel as describe before at a dose of 2 µg siRNA/disk. Disks were incubated with PBS at 37 °C in 48 well plates for 10 d. At predetermined time points, the supernatant was completely removed (250 µL) and replaced with fresh PBS solution (250 µL). The fluorescent signal of the labeled nanoparticles (fluorescein) was used to quantify nanoparticles degradation using an excitation wavelength of 490 nm and emission wavelength of 530 nm. The percentage was calculated based on the amount released at a given time point relative to the amount loaded.

In Vitro Degradation Study of PAMAM:Dextran Hydrogels: Dextran was labeled with Alexafluor-594 hydrazide (Invitrogen). Briefly, dextran (26 mg) was dissolved in distilled water and Alexafluor-594 hydrazide (2 mg) was added to the solution. The mixture was stirred at room temperature overnight in the dark. The solution was dialyzed (2 kDa molecular weight cutoff) and lyophilized. Dextran solutions containing 2%-labeled dextran were used to obtain fluorescent hydrogels doped with free siRNA or nanoparticles-encapsulated siRNA at a dose of 2 µg siRNA/disk. Disks were incubated with PBS at 37 °C in 48 well plates for 10 d, and at different time points, the solution was removed (250 µL) and replaced with fresh PBS. The collected solutions were analyzed by measuring the fluorescence intensity of Alexafluor-594 using an excitation wavelength of 590 nm and emission wavelength of 617 nm.

In Vitro Degradation of Nanoparticles: Nanoparticles-encapsulated siRNA were prepared as described before and were diluted in PBS (1 mL) and analyzed by Nanoparticle Tracking Analysis (NTA). This technique measures particle size and particle concentration by video tracking many individual particles simultaneously. Nanoparticle concentration was followed for 3 d at different time points and was indicative of nanoparticle degradation.

In Vitro Release of Alexafluor-647-Labeled siRNA from Nanoparticles: Alexafluor-647 siRNA (2 µg) was encapsulated into the nanoparticles as described before. Nanoparticles were diluted in PBS (1 mL) and were added to a dialysis bag with 2 kDa molecular weight cutoff, and incubated at 37 °C for 3 d. The fluorescent signal of released labeled siRNA (siRNA-Alexafluor-647) in 100 µL aliquots that were then replaced

DOI: 10.1002/adhm.201400235

with PBS was used to quantify siRNA release. The percentage was calculated based on the amount released at a given time point relative to the amount loaded.

In Vitro Transfection with Nanoparticles Encapsulated siGFP: Cellular transfection was performed on MDAMB231 cells stably expressing green fluorescent protein (GFP) using anti-GFP siRNA (Accell siGFPpool, Thermo Scientific). Cells were seeded at a density of 10 000 cells per well on 96 well plates, and incubated overnight to roughly 80%–90% confluence prior to conducting the transfection experiments. Polymer/siRNA nanoparticles were prepared as described before at a 200:1 ratio with RNAse-free water (Sigma). Nanoparticles were diluted in serum-free EMEM medium (ATCC) and added to cells a final concentration of 25×10^{-9} M per well. Cells were incubated for 3 h at 37 °C in 5% CO_2 atmosphere. Subsequently, cells were washed once with PBS and complete EMEM medium was added. Cells were harvested after 48 h and analyzed for GFP silencing by flow cytometry (BD LSRFortessa cell analyzer). GFP expression was compared against a negative control (untreated cells), INTERFERin Polyplus (VWR), and Lipofectamine RNAiMAX (Invitrogen) commercial transfection reagents as positive controls.

In Vitro Transfection with Hydrogel Doped with Nanoparticles Encapsulated siGFP: Cellular transfection was performed on MDA-MB-231 cells stably expressing GFP using anti-GFP siRNA (Accell siGFPpool, Thermo Scientific). Cells were seeded at a density of 50 000 cells/well on 24 well plates, and incubated overnight to roughly 80%–90% confluence prior to conducting the transfection experiments. Polymer/siRNA nanoparticles were prepared and used as described previously. Hydrogel doped with free siRNA and hydrogel doped with nanoparticles-encapsulated siRNA (Accell GFP pool) were formed as described before at a final concentration of 2 µg siRNA/disk. The disks were transferred to cell culture inserts (3 µm pore size), while cells were seeded at the bottom. After washing with PBS once, 500 µL of fresh completed medium was added to the wells and 300 µL of completed medium to the insert. Cells were harvested after 3 d and analyzed for GFP silencing by flow cytometry (BD LSRFortessa cell analyzer). GFP expression was compared with a negative control (untreated cells), and to INTERFERin Polyplus (VWR) commercial transfection reagents as positive controls.

Cell Viability Assays Post-Transfection: Cell viability assay of transfected cells was performed using the MTS assay (CellTiter 96 AQueous One Solution Cell Proliferation Assay, Promega Corporation, USA) at 48 h post-transfection with nanoparticles and 3 d post-transfection with the hydrogel as instructed by the manufacturer. Briefly, cells were transfected with Accell siGFP pool as previously described. At 48 h or 3 d post-transfection, the medium was removed, cells were washed once with PBS and complete medium supplemented with 20% MTS reagent (v/v) was added. Cells were incubated at 37 °C and absorbance was measured at 490 nm using a microplate reader (Varioskan Flash Multimode Reader, Thermo Scientific). Cell viability was expressed as relative percentage compared with untreated cells.

Mammary Fat Pad Tumor Models: Tumors in the mammary fat pad were induced in SCID mice by inoculation of MDA-MB-231 cells stably expressing firefly luciferase (Luc) (5×10^6 cells), suspended in 50 µL of HBBS solution into the mammary fat pad following a surgical incision. For determination of tumor growth, individual tumors were measured using caliper and tumor volume was calculated by: Tumor Volume (mm^3) = width × (length^2) × 2^{-1}. Treatments began when tumor volume reached about 150 mm^3. All experimental protocols were approved by the MIT Animal Care and Use Committee and were in compliance with NIH guidelines for animal use.

Treatment of Tumors with Anti-Luciferase siRNA: In vivo gene silencing efficacy was determined in SCID mice mammary fat pad tumors after injection of anti-luciferase siRNA at a dose of 10 µg per tumor. Sterile solutions, passed through 0.2 µm filters, were used to prepare fluorescent PAMAM:Dextran hydrogels (2% Alexafluor-594-Dextran) doped with nanoparticles, as described before, containing 10 µg of anti-Luc siRNA in the shape of disks (6 mm diameter, 3 mm thick). Disks were implanted next to the mammary fat pad tumor of anesthetized SCID mice. As a negative control, 100 µL of 5% glucose solution was injected directly into the tumor and as a positive control, 10 µg of anti-Luc siRNA was encapsulate with 1.6 µL JetPEI (VWR) in 100 µL 5% glucose solution and also injected intratumorally. Luciferase silencing was determined by bioluminescence measurements upon intraperitoneal (IP) luciferin administration using the Xenogen IVIS device. All experimental protocols were approved by the MIT Animal Care and Use Committee and were in compliance with NIH guidelines for animal use.

Statistical Analysis: All values are expressed as mean ± standard deviation. Statistical differences were analyzed with GraphPad Prism 5. The unpaired Student's *t*-test was used to test statistical difference between two measurements. One-way ANOVA test was used to test statistical difference between sets of measurements. *p*-Values below 0.05 were considered significant.

Supporting Information

Supporting Information is available from the Wiley Online Library or from the author.

Acknowledgements

Part of this work was supported by the Spanish Ministerio de Economia y Compaetitividad through the Grant SAF2012–39947-C02–02.

Received: May 2, 2014
Revised: June 23, 2014
Published online:

[1] T. Tokatlian, T. Segura, *Wiley Interdiscip. Rev. Nanomed. Nanobiotechnol.* **2010**, *2*, 305.
[2] Y. Wang, Z. Li, Y. Han, L. H. Liang, A. Ji, *Curr. Drug Metab.* **2010**, *11*, 182.
[3] M. S. Goldberg, D. Xing, Y. Ren, S. Orsulic, S. N. Bhatia, P. a Sharp, *Proc. Natl. Acad. Sci. U.S.A.* **2011**, *108*, 745.
[4] J. A. Wieland, T. L. Houchin-Ray, L. D. Shea, *J. Controlled Release* **2007**, *120*, 233.
[5] N. Weber, P. Ortega, M. I. Clemente, D. Shcharbin, M. Bryszewska, F. J. de la Mata, R. Gómez, M. A. Muñoz-Fernández, *J. Controlled Release* **2008**, *132*, 55.
[6] B. Ozpolat, A. K. Sood, G. Lopez-Berestein, *J. Intern. Med.* **2010**, *267*, 44.
[7] S. H. Jang, S. J. Choi, J. H. Oh, S. W. Chae, K. Nam, J. S. Park, H. J. Lee, *Drug Dev. Ind. Pharm.* **2011**, *37*, 41.
[8] P. Ofek, W. Fischer, M. Calderón, R. Haag, *FASEB J.* **2010**, *24*, 3122.
[9] A. Agrawal, D.-H. Min, N. Singh, H. Zhu, A. Birjiniuk, G. von Maltzahn, T. J. Harris, D. Xing, S. D. Woolfenden, P. a Sharp, A. Charest, S. Bhatia, *ACS Nano* **2009**, *3*, 2495.
[10] M. Stevenson, V. Ramos-Perez, S. Singh, M. Soliman, J. a Preece, S. S. Briggs, M. L. Read, L. W. Seymour, *J. Controlled Release* **2008**, *130*, 46.
[11] H. Ragelle, G. Vandermeulen, V. Préat, *J. Controlled Release* **2013**, *172*, 207.
[12] S. Y. Tzeng, B. P. Hung, W. L. Grayson, J. J. Green, *Biomaterials* **2012**, *33*, 8142.
[13] M. Cavazzana-Calvo, S. Hacein-Bey, G. de Saint Basile, F. Gross, E. Yvon, P. Nusbaum, F. Selz, C. Hue, S. Certain, J.-L. Casanova, P. Bousso, F. Le Deist, A. Fischer, *Science* **2000**, *288*, 669.
[14] G. Bajaj, M. R. Kim, S. I. Mohammed, Y. Yeo, *J. Controlled Release* **2012**, *158*, 386.

[15] Y. Wang, Z. Li, Y. Han, L. H. Liang, A. Ji, *Curr. Drug Metab.* **2010**, *11*, 182.
[16] W. J. Kim, S. W. Kim, *Pharm. Res.* **2009**, *26*, 657.
[17] A. J. Convertine, C. Diab, M. Prieve, A. Paschal, A. S. Hoffman, P. H. Johnson, P. S. Stayton, *Biomacromolecules* **2010**, *11*, 2904.
[18] H. D. Han, E. M. Mora, J. W. Roh, M. Nishimura, S. J. Lee, R. L. Stone, M. Bar-Eli, G. Lopez-Berestein, A. K. Sood, *Cancer Biol. Ther.* **2011**, *11*, 839.
[19] C. E. Nelson, A. J. Kim, E. J. Adolph, M. K. Gupta, F. Yu, K. M. Hocking, J. M. Davidson, S. A. Guelcher, C. L. Duvall, *Adv. Mater.* **2014**, *26*, 607.
[20] J. J. Green, B. Y. Zhou, M. M. Mitalipova, C. Beard, R. Langer, R. Jaenisch, D. G. Anderson, *Nano Lett.* **2008**, *8*, 3126.
[21] J. J. Green, R. Langer, D. G. Anderson, *Acc. Chem. Res.* **2008**, *41*, 749.
[22] N. Segovia, P. Dosta, A. Cascante, V. Ramos, S. Borrós, *Acta Biomater.* **2014**, *10*, 2147.
[23] C. E. Nelson, M. K. Gupta, E. J. Adolph, J. M. Shannon, S. a Guelcher, C. L. Duvall, *Biomaterials* **2012**, *33*, 1154.
[24] J. M. Saul, M. P. Linnes, B. D. Ratner, C. M. Giachelli, S. H. Pun, *Biomaterials* **2007**, *28*, 4705.
[25] M. D. Krebs, E. Alsberg, *Chemistry* **2011**, *17*, 3054.
[26] C. Achille, S. Sundaresh, B. Chu, M. Hadjiargyrou, *PLoS One* **2012**, *7*, e52356.
[27] Y. Lei, M. Rahim, Q. Ng, T. Segura, *J. Controlled Release* **2011**, *153*, 255.
[28] Y. Lei, S. Huang, P. Sharif-Kashani, Y. Chen, P. Kavehpour, T. Segura, *Biomaterials* **2010**, *31*, 9106.
[29] P. Lei, R. M. Padmashali, S. T. Andreadis, *Biomaterials* **2009**, *30*, 3790.
[30] L. Dong, Z. Huang, X. Cai, J. Xiang, Y. A. Zhu, R. Wang, J. Chen, J. Zhang, *Pharm. Res.* **2011**, *28*, 1349.
[31] S. S. Dunn, S. Tian, S. Blake, J. Wang, A. L. Galloway, A. Murphy, P. D. Pohlhaus, J. P. Rolland, M. E. Napier, J. M. DeSimone, *J. Am. Chem. Soc.* **2012**, *134*, 7423.
[32] L. Peng, X. Cheng, R. Zhuo, J. Lan, Y. Wang, B. Shi, S. Li, *J. Biomed. Mater. Res. A* **2009**, *90*, 564.
[33] N. Oliva, S. Shitreet, E. Abraham, B. Stanley, E. R. Edelman, N. Artzi, *Langmuir* **2012**, *28*, 15402.
[34] D. Oupicky, M. Ogris, K. a Howard, P. R. Dash,K. Ulbrich, L. W. Seymour, *Mol. Ther.* **2002**, *5*, 463.
[35] V. Russ, T. Fröhlich, Y. Li, A. Halama, M. Ogris, E. Wagner, *J. Gene Med.* **2010**, *12*,180.
[36] D. Trentin, J. Hubbell, H. Hall, *J. Controlled Release* **2005**, *102*, 263.
[37] P. Rujitanaroj, Y.-C. Wang, J. Wang, S. Y. Chew, *Biomaterials* **2011**, *32*, 5915.
[38] D. E. Jenkins, Y. S. Hornig, Y. Oei, J. Dusich, T. Purchio, *Breast Cancer Res.* **2005**, *7*, R444.
[39] M. Wang, A. L. Gartel, *Oncotarget* **2011**, *2*, 1218.
[40] M. D. Krebs, O. Jeon, E. Alsberg, *J. Am. Chem. Soc.* **2009**, *131*, 9204.

Adv. Healthcare Mater. **2014**,
DOI: 10.1002/adhm.201400235